Diazene (HN═NH) Is a Substrate for Nitrogenase: Insights into the Pathway of N_2 Reduction†

Brett M. Barney,‡ Jammi McClead,‡ Dmitriy Lukoyanov,§ Mikhail Laryukhin,§ Tran-Chin Yang,§ Dennis R. Dean,*,|| Brian M. Hoffman,*,§ and Lance C. Seefeldt*,‡

Department of Chemistry and Biochemistry, Utah State University, Logan, Utah 84322, Department of Biochemistry, Virginia Tech, Blacksburg, Virginia 24061, and Department of Chemistry, Northwestern University, Evanston, Illinois 60208

Received November 6, 2006; Revised Manuscript Received February 27, 2007

ABSTRACT: Nitrogenase catalyzes the sequential addition of six electrons and six protons to a N_2 that is bound to the active site metal cluster FeMo-cofactor, yielding two ammonia molecules. The nature of the intermediates bound to FeMo-cofactor along this reduction pathway remains unknown, although it has been suggested that there are intermediates at the level of reduction of diazene (HN═NH, also called diimide) and hydrazine (H_2N-NH_2). Through *in situ* generation of diazene during nitrogenase turnover, we show that diazene is a substrate for the wild-type nitrogenase and is reduced to NH_3. Diazene reduction, like N_2 reduction, is inhibited by H_2. This contrasts with the absence of H_2 inhibition when nitrogenase reduces hydrazine. These results support the existence of an intermediate early in the N_2 reduction pathway at the level of reduction of diazene. Freeze-quenching a MoFe protein variant with α-195^{His} substituted by Gln and α-70^{Val} substituted by Ala during steady-state turnover with diazene resulted in conversion of the $S = {}^3/_2$ resting state FeMo-cofactor to a novel $S = {}^1/_2$ state with $g_1 = 2.09$, $g_2 = 2.01$, and $g_3 \sim 1.98$. ^{15}N- and ^1H-ENDOR establish that this state consists of a diazene-derived [$-NH_x$] moiety bound to FeMo-cofactor. This moiety is indistinguishable from the hydrazine-derived [$-NH_x$] moiety bound to FeMo-cofactor when the same MoFe protein is trapped during turnover with hydrazine. These observations suggest that diazene joins the normal N_2-reduction pathway, and that the diazene- and hydrazine-trapped turnover states represent the same intermediate in the normal reduction of N_2 by nitrogenase. Implications of these findings for the mechanism of N_2 reduction by nitrogenase are discussed.

Nitrogenase is the enzyme responsible for catalyzing biological reduction of N_2 to two NH_3, an essential reaction in the global biogeochemical nitrogen cycle (*1*−*3*). The minimum stoichiometry for the nitrogenase catalyzed reduction of N_2 involves delivery of $8e^-$ and $8H^+$ (eq 1). The

$$N_2 + 8e^- + 16MgATP + 8H^+ \rightarrow 2NH_3 + H_2 + 16MgADP + 16P_i \quad (1)$$

Mo-based nitrogenase is composed of two component proteins called the Fe protein and the MoFe protein. The Fe protein contains a single [4Fe-4S] cluster plus two MgATP binding sites (*4*). It functions to deliver one electron at a time to the MoFe protein in a reaction coupled to the hydrolysis of the two MgATP molecules (*5*, *6*). The Fe protein dissociates from the MoFe protein after each electron transfer and hydrolysis of two MgATP (*7*), necessitating eight rounds of Fe protein binding to, and dissociation from, the MoFe protein for each N_2 reduced. The MoFe protein contains an [8Fe-7S] cluster called the P-cluster (*8*) that is proposed to mediate electron transfer between the Fe protein and the N_2-binding site, a [7Fe-9S-Mo-X-homocitrate] cluster called the FeMo-cofactor[1] (Figure 1).

Relatively little is known at a molecular level about the nitrogenase N_2-reduction mechanism beyond the fact that N_2 binds to and is reduced at one or more of the metal atoms of FeMo-cofactor (Figure 1) (*9*, *10*). It is generally accepted that the sequential addition of electrons and protons to the N_2 bound on FeMo-cofactor results in a series of semireduced and semiprotonated intermediates (*11*−*19*), ultimately yielding two ammonia molecules. In contrast to this situation, much more is known about how N_2 is activated and reduced by metal complexes (*20*). Chatt and co-workers (*21*−*23*) developed a cycle for the reduction of N_2 at a mononuclear Mo complex, with each of the key proposed intermediate states having been isolated and characterized. More recently, Schrock and co-workers (*24*−*26*) have demonstrated the catalytic reduction of N_2 to two NH_3 by a different mononuclear Mo complex, and have been able to capture and characterize many of the intermediate states along the

† This work was supported by grants from the National Institutes of Health (R01-GM59087 to L.C.S. and D.R.D.; HL13531 to B.M.H.), the National Science Foundation (MCB-0316038 to B.M.H.), and the United States Department of Agriculture Postdoctoral Fellowship program (2004-35318-14905 to B.M.B.).

* Address correspondence to these authors. L.C.S.: phone (435) 797-3964, fax (435) 797-3390, e-mail seefeldt@cc.usu.edu. D.R.D.: phone (540) 231-5895, fax (540) 231-7126, e-mail deandr@vt.edu. B.M.H.: phone (847) 491-3104, fax 847-491-7713, e-mail bmh@northwestern.edu.

‡ Utah State University.

§ Northwestern University.

|| Virginia Tech.

[1] Abbreviations: FeMo-cofactor, iron−molybdenum cofactor; EPR, electron paramagnetic resonance; ENDOR, electron nuclear double resonance.

10.1021/bi062294s CCC: $37.00
Published on Web 05/18/2007

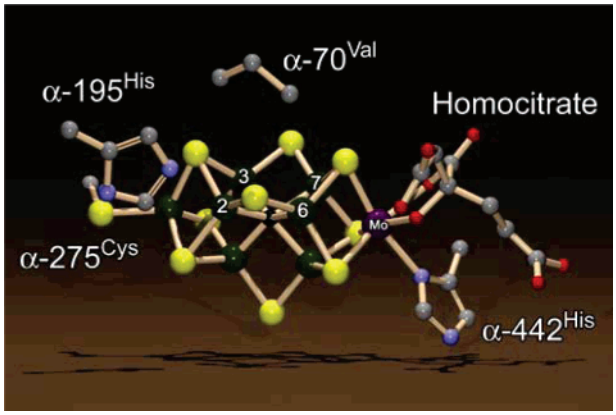

FIGURE 1: FeMo-cofactor. Shown is the structure of the FeMo-cofactor along with the side chains for a few amino acids from the MoFe protein. Fe atoms 2, 3, 6, and 7 are labeled. The color scheme is Fe in green, Mo in purple, C in gray, N in blue, O in red, and S in yellow. The atom at the center of FeMo-cofactor (X) is shown in black. The structure is based on the PDB coordinate file 1M1N and was generated using the programs DS ViewerPro and POV-ray.

reaction pathway. Both the Chatt and Schrock cycles belong to one fundamental class of potential nitrogenase mechanisms in which the first three "H atoms" (e^-/H^+) are sequentially added to a single N atom, in those instances the distal N of an end-on bound N_2, followed by cleavage of the N−N bond and release of the first NH_3 (this class of mechanisms thus has been termed "distal") (*27*). The resulting metal (M)-bound nitride (M≡N) is reduced by three additional H atoms to yield the second NH_3. In contrast to this mechanism are potential nitrogenase mechanisms in which the first five H atoms are added alternately to the two N atoms of N_2, followed by cleavage of the N−N bond and release of the first NH_3 (*27*). Reduction of the remaining metal bound amido ($-NH_2$) by a sixth H atom results in release of the second NH_3 (this class of mechanisms has been termed "alternating"). Mechanisms of the two classes begin in the same way with N_2 binding followed by the addition of two H atoms, resulting in bound isomers of diazene (M−N═NH). The mechanisms then diverge, with distal mechanisms having nitride (M≡N) and imido (M═NH) intermediates, while the alternating mechanisms include hydrazido (M−NH═NH_2) and hydrazine (M−NH_2−NH_2) intermediates. The two mechanism classes then converge to an amido (M−NH_2) state.

A major goal of nitrogenase research is to devise experiments to characterize the reaction intermediates during N_2 reduction and thereby to determine the mechanism and its molecular details. Within the framework of the alternating class of mechanisms, a reasonable starting assumption is that the nitrogenase reaction mechanism for N_2 reduction involves intermediates in which the FeMo-cofactor (denoted as M) binds N_2-derived species at the levels of reduction of diazene (N_2H_2) and hydrazine (N_2H_4) (eq 2). This view was supported

$$M + N_2 \rightarrow M-N_2 \rightarrow M-N_2H_2 \rightarrow M-N_2H_4 \rightarrow 2NH_3 + M \quad (2)$$

by the early demonstration that hydrazine (H_2N-NH_2) is a substrate for nitrogenase, and is reduced by two electrons and two protons to yield two ammonia molecules (*28*). The assumption is that hydrazine joins into a late step in the same reaction pathway utilized during N_2 reduction (*11*).

Despite these observations, little is known at the molecular level about the nature of N_2-reduction intermediates actually bound to nitrogenase. While a FeMo-cofactor bound diazene seems likely as an early intermediate in the pathway, assessment of the interactions of diazene with nitrogenase has proven challenging because of the short half-life of diazene in aqueous solutions. McKenna and co-workers (*29*, *30*) were able to demonstrate that dimethyldiazene ($H_3C-N═N-CH_3$) and diazirine (cyclic methyldiazene) are substrates for nitrogenase. More recently it was shown that methyldiazene ($HN═N-CH_3$) could be used as a substrate for nitrogenase (*27*). An intermediate was trapped during turnover of this substrate, and ENDOR spectroscopy was used to show that it contains a methyldiazene-derived [$-NH_x$] species bound to FeMo-cofactor. While the results obtained so far have been important in understanding early steps in the nitrogenase mechanism, the fact that they are obtained with diazene analogues requires extrapolation to the N_2-reduction mechanism.

Here, we employ the *in situ* generation of diazene itself to demonstrate that it is a nitrogenase substrate that is reduced to ammonia. Moreover, it is shown that the reduction of both N_2 and diazene is inhibited by H_2, indicating that diazene enters at an early step in the same reaction pathway. By substitution of amino acids in the MoFe protein near FeMo-cofactor, it has been possible to trap an intermediate in which a diazene-derived species is bound to FeMo-cofactor, and to establish the properties of this bound state by X/Q-band EPR and Q-band ^{15}N-ENDOR spectroscopies. The properties of this diazene-derived state are directly compared to those of a hydrazine-derived state trapped during turnover. The features of diazene reduction by nitrogenase along with the properties of the diazene-derived intermediate provide new insights into the nitrogenase N_2 reduction mechanism.

MATERIALS AND METHODS

Materials and Proteins. All reagents were obtained from Sigma-Aldrich Chemicals (St. Louis, MO) and were used as supplied unless stated otherwise. ^{15}N-labeled hydrazine was obtained from Cambridge Isotopes (Andover, MA). *Azotobacter vinelandii* strains DJ995 (wild-type MoFe protein), DJ1310 (α-70^{Ala} MoFe protein), DJ997 (α-195^{Gln} MoFe protein), and DJ1316 (α-195^{Gln}/α-70^{Ala} MoFe protein) were constructed and nitrogenase proteins were expressed and purified as described previously (*31*). All proteins used were greater than 95% pure as judged by SDS−PAGE analysis using Coomassie blue staining. Manipulation of proteins was done in septum-sealed serum vials under an argon atmosphere. All transfer of gases and liquids was done using gastight syringes.

Azodiformate Synthesis. Azodiformate (**5** in Figure 2) is the precursor for diazene production. It is prepared from azodicarbonamide (**4** in Figure 2) using the procedure of Graham Palmer (*32*), with slight modifications. Preparation of azodicarbonamide (**4**) was accomplished after first synthesizing biurea (**3** in Figure 2) using the procedure of Audrieth and Mohr (*33*). The synthesis began with 200 mg of ^{14}N- or ^{15}N-labeled hydrazine sulfate (**1** in Figure 2) dissolved in a 3 mL solution of 0.5 M acetic acid in water. To this solution was added dropwise 275 mg of potassium cyanate (**2** in Figure 2) dissolved in 0.93 mL of water. The

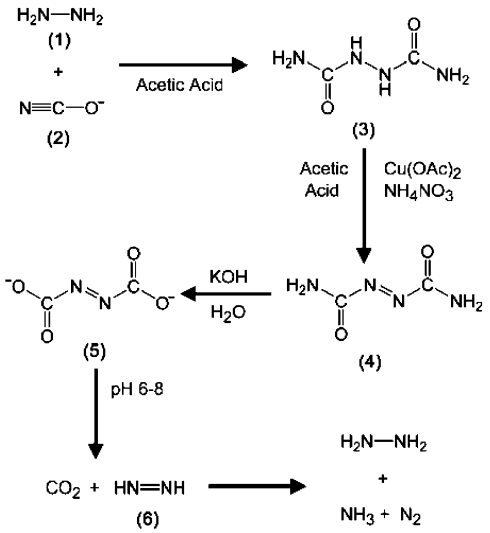

FIGURE 2: Diazene synthetic scheme. Biurea (**3**) was synthesized as a white precipitate following reaction of hydrazine (**1**, where the N atoms were either ^{14}N or ^{15}N) and cyanate (**2**). Biurea (**3**) was oxidized by copper acetate yielding the orange precipitate azodicarboamide (**4**). This was treated with base to form azodiformate (**5**). Neutralization of azodiformate (**5**) by addition to the buffered assay mixture rapidly yielded diazene (**6**) and CO_2. The breakdown of diazene to hydrazine, N_2, and ammonia is also shown. See Materials and Methods for details.

mixture was stirred gently for 4 h at room temperature and then transferred to a 25 mL centrifuge tube. The biurea (**3**) product was crystallized by the addition of 2 mL of water and isolated as a white precipitate collected by centrifugation at 5000*g* for 5 min. The precipitate was washed twice with absolute ethanol followed by diethyl ether (2 mL each wash) with a yield of 150 mg. After being dried under vacuum for several minutes, the biurea (**3**) was used in the synthesis of azodicarbonamide (**4** in Figure 2). The biurea was oxidized to azodicarbonamide using cupric acetate and nitrate following the procedure of Kepler (*34*). Biurea (150 mg) was added to a 3.25 mL solution of glacial acetic acid containing 3 mg of cupric acetate. This was followed by the addition of 146 mg of ammonium nitrate (solid). The resulting solution was refluxed at 115 °C for 10 min and then cooled to 45 °C. The azodicarbonamide (**4**) was isolated as an orange precipitate collected by centrifugation and was washed several times with cold water, yielding 100 mg of product with a calculated yield of ~70%. The azodicarbonamide (**4**) was dried overnight under vacuum and stored at room temperature. The azodicarbonamide (**4**) was dissolved in 2 mL of half-saturated KOH solution in H_2O (about 2 g in 4 mL of H_2O), generating azodiformate (**5**), which was then precipitated by adding ethanol (~20 mL). This was washed with 50% ether in ethanol, and then dried overnight under vacuum, giving a yield of ~90%. Dried azodiformate (**5**) was stable for many weeks when stored under argon in the dark.

Nitrogenase Activity Assays. Substrate reduction reactions for nitrogenase proteins were conducted at 30 °C using a variation of a method described previously (*35*). The assay solution contained a MgATP regeneration system (5 mM ATP, 6 mM $MgCl_2$, 30 mM phosphocreatine, and 0.2 mg/mL creatine phosphokinase) in MOPS buffer (200 mM, pH 7.2) with 1.2 mg/mL bovine serum albumin and 9 mM sodium dithionite. Solutions were degassed with oxygen-free argon and brought to a final pressure of 1 atm prior to the addition of dithionite. MoFe protein (200 μg) was added followed by Fe protein (500 μg) to initiate the reaction. Reactions proceeded with shaking at 30 °C and were then quenched by the addition of 300 μL of 400 mM EDTA. Concentrations of azodiformate were established using the extinction coefficient of 33 M^{-1} cm^{-1} at 403 nm (*32*). A 500 mM azodiformate (**5** in Figure 2) stock solution (made in a 150 mM KOH solution in water) was prepared just prior to starting the assay, and 5−50 μL of this solution was added to the assay solution immediately following initiation of the reaction by addition of the Fe protein. Upon addition of the azodiformate (**5**) solution to the assay solution, with the neutralization of the pH, an immediate reaction occurred, yielding the gases diazene and carbon dioxide. The quantity of diazene is presented as equal to the quantity of azodiformate added, although it is clear that the real concentration of diazene will always be lower than this value. Adding the same quantity of a 150 mM KOH solution without azodiformate to an assay had no noticeable affect on the proton reduction activity or pH of the solution.

Where indicated, the gases nitrogen, argon, or acetylene were added as an overpressure, and the vial was then vented to 1 atm final pressure. Hydrogen was quantified by gas chromatography. Ammonia was quantified using a fluorescence detection method (*36*) with slight modifications. A 25 μL aliquot of postreaction solution containing NH_3 was added to 1 mL of a solution containing 20 mM phthalic dicarboxyaldehyde, 3.5 mM 2-mercaptoethanol, and 5% (v/v) ethanol in a 200 mM potassium phosphate buffer, pH 7.3, and allowed to react in the dark for 30 min. The fluorescence ($\lambda_{excitation}/\lambda_{emission}$ 410 nm/472 nm) of the mixture was used to quantify ammonia by comparison to a standard made using NH_4Cl, using a Shimadzu model RF-5301 PC spectrofluorometer and the software provided with the instrument.

Hydrazine was quantified using a previously reported colorimetric assay (*11*). Briefly, 5 μL of sample or standard (up to 5 mM) was added to a disposable 1 mL cuvette. Then 1 mL of the assay solution, containing 70 mM dimethylaminobenzaldehyde and 1 M HCl in 95% ethanol, was added to the cuvette, and allowed to sit for 15 min. The absorbance at 458 nm was then used to quantify amounts of hydrazine versus a blank and a standard curve prepared from hydrazine sulfate.

X-band EPR Sample Preparation and Analysis. EPR samples were prepared in a solution containing a MgATP regeneration system (10 mM ATP, 15 mM $MgCl_2$, 20 mM phosphocreatine, and 0.2 mg/mL phosphocreatine kinase) in 150 mM MOPS buffer, pH 7.3, with 50 mM dithionite. MoFe protein was added to a final concentration of ~75 μM. Azodiformate was added from a stock solution (described above). Turnover conditions were initiated by the addition of Fe protein to a final concentration of 50 μM. EPR samples under resting conditions were prepared as described above, except that Fe protein was not included. All X-band EPR samples were frozen in 4 mm calibrated quartz EPR tubes at 77 K. For the pH profile, the same solution as described above was used, except that the buffer was 50 mM MES, 50 mM TAPS, and 50 mM MOPS and the pH was adjusted by the addition of HCl or NaOH. X-band EPR spectra were recorded using a Bruker ESP-300 E spectrometer with an ER 4116 dual-mode X-band cavity equipped with an Oxford

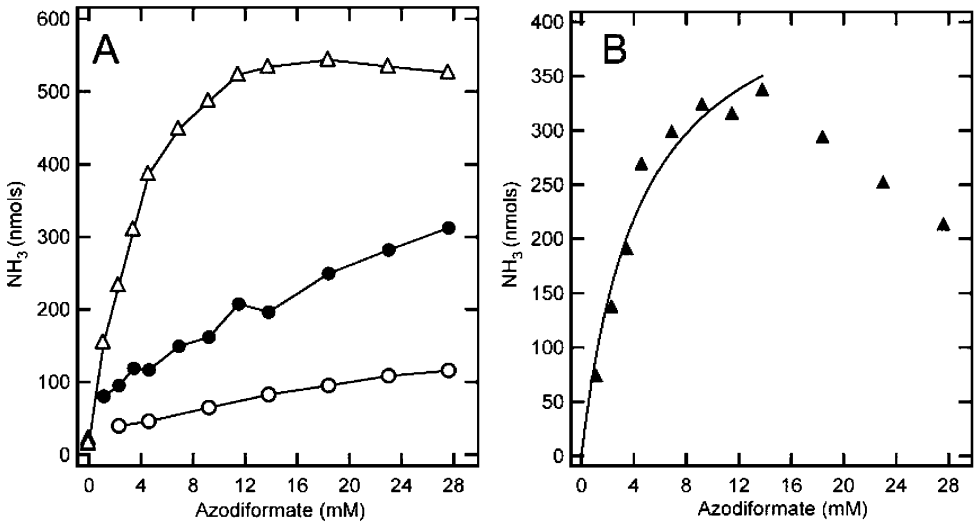

FIGURE 3: Diazene is a substrate for nitrogenase. (A) Total ammonia detected following 5 min of reaction with 200 μg (800 nM) of wild-type MoFe protein and 500 μg (8 μM) of Fe protein in a total assay solution volume of 1 mL is shown as a function of the concentration of azodiformate added (△). Also shown is the total ammonia detected for a similar assay condition except that EDTA was added before initiation of the reaction (○), and for an assay where azodiformate was added 30 min prior to the initiation of the enzyme reaction by addition of the Fe protein (●). (B) The total ammonia detected minus the ammonia assigned to non-nitrogenase catalyzed diazene breakdown and from non-diazene sources is plotted against the concentration of azodiformate added (▲). The points up to 15 mM azodiformate are fitted to the Michaelis−Menten equation (line).

Instruments ESR-900 helium flow cryostat. Spectra were obtained at a microwave frequency of ~9.65 GHz. Precise values of the frequency were recorded for each spectrum to determine proper *g* alignment. Initial spectra were obtained at a microwave power of 1.0 mW, with a modulation amplitude of 1.26 mT and a temperature of 8 K and were the sum of five scans. Subsequent data manipulation was done using IGOR Pro (WaveMetrics, Lake Osewego, OR). The temperature-dependence (4.8 to 14 K) of the EPR signal intensity was determined at 100 μW for the turnover and resting state signals. The microwave power dependence on EPR signal intensity was determined at 4.8 K with microwave powers ranging from 10 μW to 2 mW.

35 GHz EPR/ENDOR Spectroscopy. Q-band samples were prepared as described above (*39*), except that the MoFe protein concentration was ~200 μM, and the reactions were initiated by addition of 100 μM of Fe protein. CW and Mims/ReMims pulsed 35 GHz ENDOR spectra were recorded at 2 K on spectrometers described previously (*37*). The ENDOR pattern for an $I = {}^1/_2$ nucleus (^{1}H, ^{15}N) exhibits a $\nu(\pm)$ doublet that is split by the hyperfine coupling, *A*, and centered at the nuclear Larmor frequency. The Mims pulse sequence, $[\pi/2-\tau-\pi/2-\mathrm{T(rf)}-\pi/2-\mathrm{detect}]$, has the property that its ENDOR intensities follow the relationship, $I(A) \sim 1 - \cos(2\pi A\tau)$ (*38*). As a result, the signals vanish ("blind spots') at $A\tau = n$, $n = 0, 1, ...$, and show maximum intensities at $A\tau = n + {}^1/_2$. The ReMims sequence $[\pi/2-\tau_1-\pi/2-\mathrm{T(rf)}-\pi/2-\tau_2-\pi-\mathrm{detect}]$ is used to overcome spectrometer dead-time limitations (*40*), and to place all "blind spots" with $n > 0$ at frequencies that are outside the ENDOR envelope.

RESULTS

Diazene Is a Substrate for Nitrogenase. Despite the obvious importance of studying the reactions of diazene (**6** in Figure 2) with nitrogenase, the short half-life of diazene in aqueous solutions (*41*) has made such studies difficult. Diazene undergoes both dismutation (eq 3) and decomposition (eq 4) reactions near neutral pH, with an estimated half-life at pH 8.0 of 5 s (*32*, *41*). Despite this short half-life,

$$2N_2H_2 \rightarrow N_2H_4 + N_2 \quad (3)$$

$$2N_2H_2 + 2H^+ \rightarrow 2\,H_2 + N_2 \quad (4)$$

however, it was shown that diazene can be generated more rapidly than it decays, thus allowing a steady-state concentration of diazene to accumulate in solution for short times (<30 s) (*32*). This is achieved by rapidly generating diazene by neutralization of azodiformate (**5** in Figure 2). Azodiformate (**5**), which is synthesized from azodicarbonamide (**4** in Figure 2) in KOH, is stable at room temperature when dry or for several hours when maintained at high pH. Upon neutralization of azodiformate (**5**) by adding a small quantity to an enzyme solution buffered near neutral pH, diazene and CO_2 are rapidly liberated. This strategy was successfully employed to investigate the interaction of diazene with cytochrome *c* oxidase (*32*).

Here, we have similarly generated diazene in solution with nitrogenase under turnover conditions as a way to probe diazene as a possible substrate, inhibitor, and ligand. An important issue was to distinguish diazene interactions with nitrogenase from the possible interactions of diazene decay products (e.g., N_2 and hydrazine). When nitrogenase is allowed to turn over (MoFe and Fe proteins, reductant, MgATP, and MgATP regeneration system) for 5 min in the presence of different concentrations of diazene (added as azodiformate[2]), total ammonia production is seen to increase with increasing diazene concentration, with saturation observed at the highest concentrations (Figure 3A, upper curve).

[2] Throughout, all reference to the quantity of diazene added actually represents the corresponding quantity of azodiformate added. The actual quantity of diazene present will be lower.

It was important to determine how much of this ammonia production might be coming from nitrogenase reduction of diazene and how much was coming from other sources, such as the decomposition of diazene that is not catalyzed by nitrogenase. The latter contribution to the ammonia detected was established by repeating the turnover experiment except that the nitrogenase reaction quencher EDTA had been added to the assay at the beginning of the reaction before azodiformate was added. As can be seen in Figure 3A (lower curve), ammonia was detected under these conditions arising from nonenzymatic decay of diazene, but the quantity was much lower than that observed from the enzyme-catalyzed reaction.

The other potential source of ammonia in these assays would be nitrogenase reduction of diazene breakdown products (e.g., N_2 and hydrazine). To establish the maximum contribution to ammonia production from nitrogenase reduction of diazene breakdown products, an assay was conducted where azodiformate was added 30 min prior to the initiation of the enzyme catalyzed reaction. In this case, the diazene would fully decompose prior to initiation of the assay (*32*, *41*). Nitrogenase added after the 30 min preincubation was then allowed to react for 5 min prior to quenching with EDTA (Figure 3, middle curve). The ammonia produced under these conditions results from the breakdown of diazene directly to ammonia and from nitrogenase reduction of diazene breakdown products. This ammonia production represents the upper limit to the amount of ammonia produced during normal diazene turnover that does not come from nitrogenase reduction of diazene itself.

The difference between the ammonia production in the presence of diazene and that ascribed to non-diazene and non-nitrogenase reactions represents the ammonia produced from nitrogenase reduction of diazene. This corrected ammonia production from nitrogenase reduction of diazene is plotted as a function of diazene (azodiformate) concentration (Figure 3B). It is evident that nitrogenase reduces diazene to ammonia in a concentration-dependent reaction, with saturation at approximately 12 mM diazene (added azodiformate). It is noted that, at still higher concentrations of diazene, inhibition of diazene reduction to ammonia is observed. This inhibition could reflect competition for the nitrogenase active site from N_2 and hydrazine (breakdown products of diazene) or from substrate inhibition. For the lower concentrations of diazene, the data were fit to the Michaelis−Menten equation to obtain estimates of kinetic parameters for nitrogenase reduction of diazene. While it is not possible to establish an accurate V_{max} and K_m for diazene because the substrate concentration is changing during the course of the assay, it is possible to obtain limits. From the results in Figure 3B, a minimum V_{max} for diazene reduction by nitrogenase is found to be 400 nmol of NH_3/min/mg of MoFe protein. This value compares favorably with the V_{max} for N_2 reduction by nitrogenase determined in a parallel experiment of 600 nmol of NH_3/min/mg of MoFe protein (*35*). Likewise, an upper limit on the K_m for diazene is calculated to be 4.5 mM, compared to the K_m for N_2 of 60 μM (*35*).

Hydrogen Inhibits Diazene Reduction by Nitrogenase. An important mechanistic aspect of N_2 reduction by nitrogenase is that this reaction is inhibited by H_2 (*1*, *10*, *42*). Several proposals have been put forward to explain this inhibition, with all sharing the assumption that H_2 and N_2 interact with the same or similar sites and reduction states of FeMo-cofactor (*1*, *10*, *43*). Consistent with this proposal is the observation that H_2 does not inhibit hydrazine reduction, which is presumed to occur later in the N_2 reduction pathway. Likewise, H_2 does not inhibit reduction of nonphysiological substrates such as acetylene (results for acetylene and hydrazine are shown in Table 1).

Table 1: Inhibition of Substrate Reduction by H_2

additions[a]	sp act. (nmol of NH_3 or C_2H_4/min/mg)[b]	% inhibn of maximal act.
0.11 atm of N_2[c]	172 ± 15	
0.11 atm of N_2, 0.89 atm of H_2	63 ± 4	63
4.6 μmol of azodiformate[d]	373 ± 36	
4.6 μmol of azodiformate, 1 atm of H_2	189 ± 7	58[d]
10 mM hydrazine[e]	540 ± 10	
10 mM hydrazine, 1 atm H_2[c]	530 ± 5	2
0.01 atm of acetylene[c]	770 ± 16	
0.01 atm of acetylene, 1 atm of H_2	755 ± 17	2

[a] Gases are added as a partial pressure with argon added to achieve 1 atm total pressure. [b] Ammonia and ethylene were quantified as described in the Materials and Methods section. [c] Nitrogen and acetylene reduction assays were performed at pH 7.0 for 10 min using 100 μg of MoFe protein. [d] Diazene reduction assays were performed at pH 7.0 for 5 min using 200 μg of MoFe protein. [e] Hydrazine reduction assays were performed at pH 7.2 for 10 min using 200 μg of the α-70^{Ala} MoFe protein.

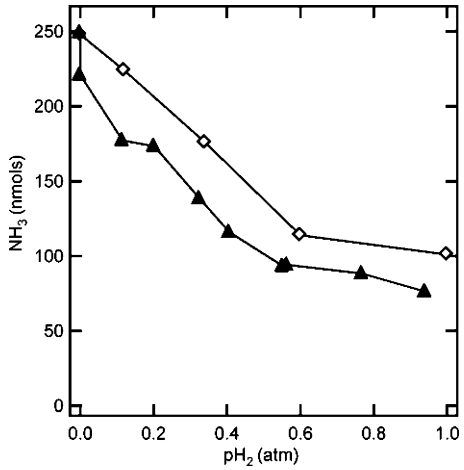

FIGURE 4: Hydrogen inhibition of diazene and nitrogen reduction. The quantity of amnmonia detected after 5 min of turnover under N_2 (▲) or diazene (◇) is shown as a function of the partial pressure of H_2 (pH_2) with Ar as the supplementary gas. Assay conditions were as described in the legend to Figure 3.

When H_2 was included in a diazene reduction assay, significant inhibition of ammonia production (corrected to ammonia production from diazene reduction by nitrogenase) was observed (Table 1). The extent of H_2 inhibition of diazene reduction was similar to that seen for H_2 inhibition of N_2 reduction under these conditions. Figure 4 shows the effects of increasing H_2 partial pressure on nitrogenase-catalyzed ammonia production from either N_2 or diazene. It can be seen that H_2 inhibition of diazene reduction parallels the H_2 inhibition of N_2 reduction. Thus, N_2 and diazene behave alike, and differently from hydrazine or acetylene, in that their reduction by nitrogenase is inhibited by H_2.

Diazene Inhibits Proton Reduction. Like any other substrate for nitrogenase, diazene should compete for electron

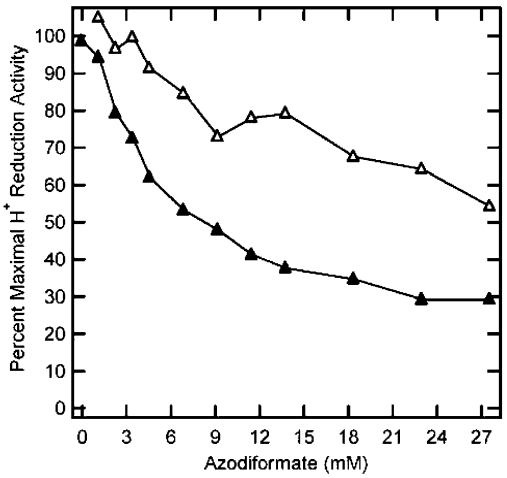

FIGURE 5: Diazene inhibition of proton reduction. The percentage of the maximum proton reduction activity of wild-type MoFe protein is plotted against the concentration of azodiformate added for a reaction where azodiformate is added upon initiation of the reaction (▲) and when the reaction is initiated 30 min after addition of azodiformate (△). Assay conditions were as described in the legend to Figure 3.

flux through nitrogenase (*1*). Thus, it is expected that, in the presence of diazene, the rate of H_2 formation by nitrogenase should decrease as electrons are diverted to the competing substrate. Figure 5 shows the effects of increasing diazene concentration on the H_2 evolution rate catalyzed by nitrogenase. The open symbols represent the H_2 production rates observed when diazene is allowed to decompose prior to the initiation of the assay, and thus accounts for all non-diazene inhibitors and substrates. The lower (closed) data represent the H_2 reduction rates when diazene is present. From the difference between these curves, it is apparent that diazene inhibits H_2 evolution by nitrogenase, indicating competition for electron flux through nitrogenase.

Trapping a Diazene-Derived Species Bound to FeMo-Cofactor. Given that diazene is a substrate for nitrogenase, we attempted to trap an intermediate with a diazene-derived species bound to FeMo-cofactor, as this might represent an early state along the reaction pathway. The trapping of substrate-derived species on FeMo-cofactor can be monitored by the change in the EPR spectrum of the FeMo-cofactor (*27*, *36*, *44*−*49*). In its resting state (called M^N), FeMo-cofactor is in an $S = {}^3/_2$ spin state with a characteristic EPR spectrum in the perpendicular mode with *g* values of 4.45, 3.56, and 2.00 (Figure 6). When nitrogenase is freeze-trapped under proton reduction conditions, this EPR signal is greatly diminished in intensity, which has been interpreted as the conversion of FeMo-cofactor to a more reduced, diamagnetic state (called M^R) (*50*, *51*). When the wild-type MoFe protein is freeze-trapped during turnover with diazene, the $S = {}^3/_2$ resting-state FeMo-cofactor EPR signal partially converts to a new state with an $S = {}^1/_2$ EPR signal (Figure 6). However, based on its *g* values, this appears to be from an N_2-turnover state, probably formed with N_2 generated as a breakdown product of diazene (*49*). In contrast, conversion to an intermediate with a distinct EPR signal is observed when the α-195^{Gln} MoFe protein is trapped during turnover with diazene; the substitution of α-195^{His} by Gln has been suggested to limit proton delivery for reduction of nitrogenous substrates, and thus to arrest the reduction of these

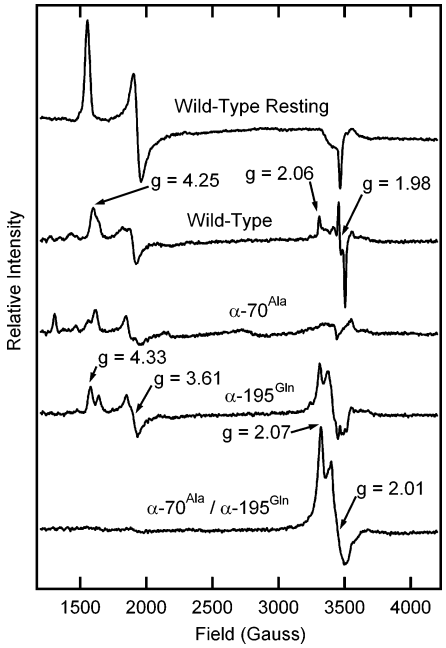

FIGURE 6: EPR spectra for various MoFe proteins trapped with diazene. Shown are X-band EPR spectra for the wild-type MoFe protein in the resting state (top trace) and other MoFe proteins (15 μM) trapped by freezing during turnover in the presence of 5 μmol of azodiformate in a total liquid volume of 400 μL at pH 6.5. Turnover and EPR conditions are described in the Materials and Methods section.

substrates (*36*, *52*, *53*). The further substitution of α-70^{Val} by Ala in the α-195^{Gln} MoFe protein (double substituted MoFe protein) leads to a more complete conversion of the resting-state FeMo-cofactor EPR signal to the new $S = {}^1/_2$ state. Substitution of α-70^{Val} by Ala has been shown to open up the nitrogenase active site, allowing larger substrates to interact (*54*).

It was important to establish that the trapped state observed by EPR is a result of diazene binding to or reacting with nitrogenase, and not one of the diazene breakdown products. In an experiment parallel to the kinetic studies described above, diazene was allowed to decompose for 30 min in an EPR tube prior to the addition of the nitrogenase proteins. Following the addition of nitrogenase proteins, the reaction mixture was allowed to react for 30 s before being frozen in liquid nitrogen. The EPR spectrum of this sample was compared to the spectrum obtained when nitrogenase proteins were added to the reaction solution immediately after generating the diazene (Figure 7). It is evident that most of the new $S = {}^1/_2$ EPR spectrum observed when nitrogenase is trapped during turnover with diazene results from nitrogenase interaction with diazene rather than with a diazene breakdown product.

The X-band EPR signal of the diazene-trapped state of α-195^{Gln}/α-70^{Ala} MoFe protein appears axial. To increase the *g*-resolution for comparison between the diazene- and hydrazine-trapped states, EPR spectra were collected at Q-band. Figure 8 presents a Q-band absorption-display EPR spectrum of the diazene-trapped state and its derivative, each overlaid with the corresponding EPR spectra of the hydrazine-trapped state in the same α-70^{Ala}/α-195^{Gln} MoFe protein. Overall, the spectra of the intermediates are highly similar, and again appear to be axial, with $g_\perp = 2.01$ and $g_\parallel \sim 2.1$. Although, there is interference in the low-*g* region from the

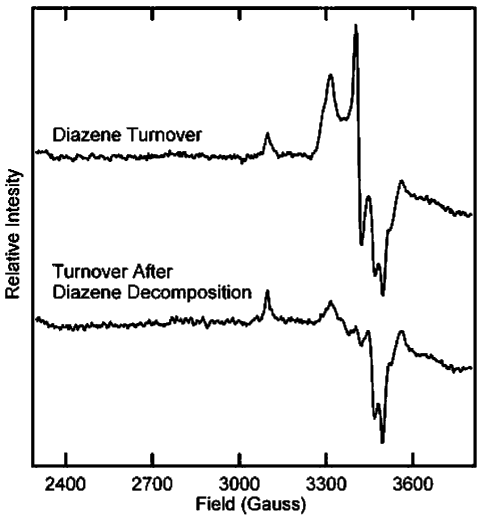

FIGURE 7: EPR spectra for α-70^{Ala}/α-195^{Gln} MoFe protein trapped with diazene or diazene decomposition products. Shown are X-band EPR spectra for the α-70^{Ala}/α-195^{Gln} MoFe protein trapped during turnover with 4 mM azodiformate (upper trace) or trapped during turnover with 4 mM azodiformate that was allowed to decompose for 30 min prior to the initiation of the reaction (lower trace). Turnover and EPR condition are described in the Materials and Methods section.

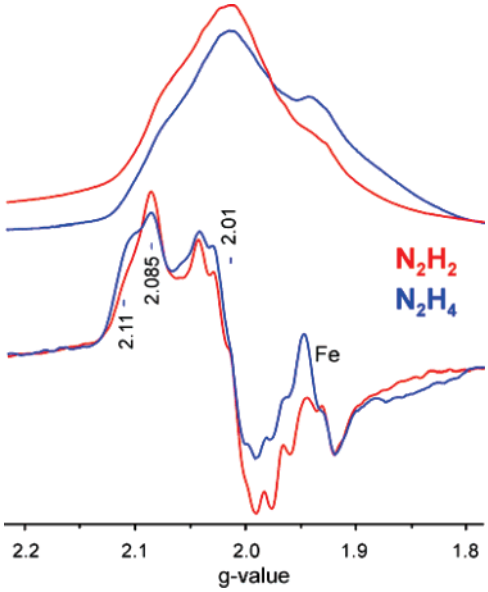

FIGURE 8: Q-band EPR spectra of diazene- and hydrazine-dependent intermediates. (Upper traces) Absorption-display rapid-passage spectra. (Lower traces) Digital derivatives. These enhance the tiny signal from adventitious Mn^{2+}. Conditions: microwave frequency, 35.025−35.041 GHz; microwave power, ~ 1 mW; modulation amplitude, 1.3 G; sweep rate, 33 G/s; time constant, 128 ms; temperature, 2 K.

Fe protein EPR signal at $g = 1.93$, the collection of ENDOR spectrum over a range of fields (not shown) suggests that the spectra of both intermediates in fact have a rhombic splitting, with $g_2 = 2.01$ and $g_3 \leq 1.98$. The shapes of the $g_1 \sim 2.1$ features of the spectra further suggest that both intermediates are heterogeneous. Spectra taken over a range of incident microwave powers (see Supporting Information, Figure S1) confirm that the signal of each intermediate is a superposition of spectra with $g_{||} = 2.11$ and $g_{||} = 2.085$, presumably from two major substates with slightly different properties; the $g_{||} = 2.085$ conformation dominates in the diazene-derived intermediate whereas the two have comparable contributions in the hydrazine-derived intermediate. Quantification of the diazene-dependent EPR signal by comparison to a CuEDTA standard solution indicates that this signal represents ~60% spin conversion of FeMo-cofactor.

The pH dependence of the intensities of the EPR signals of the diazene- and hydrazine-derived intermediates were determined (see Supporting Information, Figure S2). The EPR signal of the diazene-trapped state was most intense at the lowest pH values and declined in intensity as the pH rose. For the hydrazine-trapped state, the intensity of the EPR signal rose to a maximum at pH 7.5 and then declined in intensity at higher pH values. The microwave power dependence of the diazene- and hydrazine-derived EPR signal intensities also was determined, and found to be nearly identical (see Supporting Information, Figure S3).

^{15}N,^{1}H-ENDOR. To establish if the diazene-trapped state contained a diazene-derived species bound to FeMo-cofactor, Q-band ^{15}N pulsed Mims and ReMims ENDOR were used on nitrogenase with ^{15}N-labeled diazene trapped (Figure 9A). $^{15}N_2H_2$ was prepared by first synthesizing biurea (**3** in Figure 2) from ^{15}N-hydrazine (**1** in Figure 2). The biurea (**3**) was oxidized to azocarboamide (**4**), which in turn could be readily converted to azodiformate (**5**). The ^{15}N-azodiformate was used to generate ^{15}N-diazene as outlined above, and the α-70^{Ala}/α-195^{Gln} MoFe protein was freeze-trapped during turnover with this substrate. To test whether this state is the same as the hydrazine-derived state, the α-195^{Gln}/α-70^{Ala} MoFe protein also was trapped with $^{14,15}N_2H_4$.

Selected ^{15}N-ENDOR spectra for the diazene-dependent state and for the hydrazine-dependent state are shown at fields near to the common principal g-values (Figure 9A). Spectra collected over a wider frequency range (not shown) revealed no additional signals from ^{15}N with larger couplings for either sample; neither were additional signals with smaller hyperfine couplings detected through lengthening of the interpulse spacing to $\tau = 800$ ns, which accentuates smaller couplings (see Materials and Methods).

The single-crystal-like spectra for the two states, collected at a field corresponding to $g_{||} = 2.09$, show a doublet from a single (type of) ^{15}N, centered at the ^{15}N Larmor frequency and split by the ^{15}N hyperfine coupling, $A = 1.80(4)$ MHz. The individual peaks broaden and show additional resolved features as the field is increased, a consequence of an anisotropic contribution to the hyperfine tensor. As the spectra for the two states are indistinguishable at all fields, we conclude that the hyperfine tensors of the ^{15}N that give rise to the signals are identical for the substrate-derived species bound to FeMo-cofactor in the two intermediates.

A combination of ^{15}N- and ^{1}H-ENDOR measurements showed that the hydrazine-derived species binds to FeMo-cofactor through an [−NH_x] moiety (*36*, *49*). To complete the comparison between the diazene and hydrazine-derived states, each was prepared in H_2O or D_2O solvents and CW and Davies pulsed ^{1}H-ENDOR spectra were collected at $g = 2.04$ and $g_2 = 2.018$, respectively (Figure 9B**)**. These were collected under conditions yielding higher resolution than the original CW spectra for hydrazine. The spectra for both states reveal an unresolved, nonexchangeable (unchanged in D_2O buffer) matrix ^{1}H peak at the proton Larmor frequency, as well as resolved shoulders from nonexchangeable proton(s) with coupling, $A \sim 4.5$ MHz. In addition, the spectra

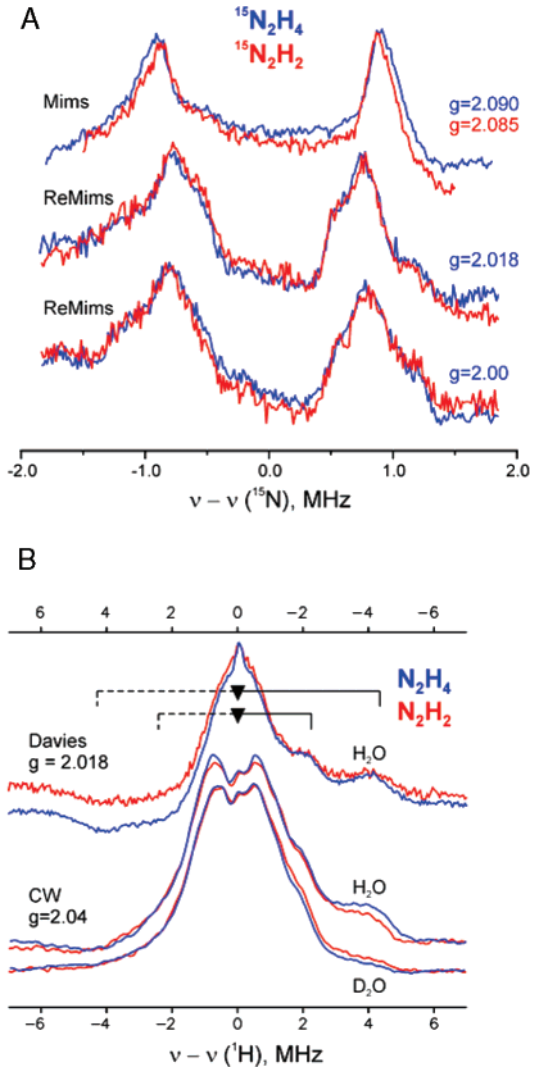

FIGURE 9: ENDOR spectra. (A) Comparison of pulsed ^{15}N-ENDOR spectra for α-70^{Ala}/α-195^{Gln} MoFe protein trapped during turnover with diazene (red) or hydrazine (blue). Conditions: Mims sequence, $\pi/2 = 52$ ns, $\tau = 300$ ns, RF 20 μs, 50 shots/point, 10 scans, 2 K, (N_2H_4) $g = 2.09$, 34.776 GHz, 20 ms repetition rate, and (N_2H_2) $g = 2.085$, 34.702 GHz, 10 ms repetition rate; ReMims sequence, $\pi/2 = 32$ ns, $\tau_1 = 224$ ns, RF 20 μs, 50 shots/point, 10 ms repetition rate, 2 K, (N_2H_4) 34.776 GHz, 20 scans, and (N_2H_2) 34.768 GHz, 40 scans. (B) Comparison of pulsed (upper axis) and CW (lower axis) ^{1}H-ENDOR spectra for α-70^{Ala}/α-195^{Gln} MoFe protein trapped during turnover with diazene (red) or hydrazine (blue) in H_2O and D_2O buffers. Resolved hyperfine couplings to exchangeable (8.5 MHz) and nonexchangeable (4.5 MHz) proton(s) are indicated by braces. The asymmetry of the spectra reflect relaxation effects; these effects are of opposite senses for pulse and CW, hence the Davies spectra are plotted from high to low frequency. Conditions: Davies, $g = 2.018$, $\pi/2 = 40$ ns, $\tau = 560$ ns, RF 40 μs, 50 shots/point, 10 ms repetition rate, (N_2H_4) 34.712 GHz, 18 scans and (N_2H_2) 34.730 GHz, 30 scans; CW ENDOR, 35.071−35.129GHz, modulation amplitude = 1.3 G, time constant = 64 ms, RF sweep speed = 1 MHz/s, bandwidth of RF broadened to 100 kHz, 2 K.

showed the signal seen earlier from an exchangeable proton(s) with $A \sim 8.5$ MHz. As discussed, this coupling is most plausibly assigned to an [−NH_x] moiety bound directly to the FeMo-cofactor.

DISCUSSION

The rapid *in situ* generation of diazene directly in a nitrogenase reaction solution permitted an assessment of the interaction of this unstable compound with nitrogenase. Using this strategy, it was possible to demonstrate that diazene is a substrate for nitrogenase, being reduced to ammonia. Given the instability of diazene in solution (*32*, *41*), it was essential to establish that diazene was the principal substrate rather than a breakdown product. In fact, a fraction of the total ammonia observed in a nitrogenase turnover reaction in the presence of diazene can be ascribed to nonenzymatic diazene decomposition to ammonia in addition to nitrogenase reduction of diazene decomposition products (N_2 and hydrazine). However, the significant additional ammonia production can only be assigned to nitrogenase reduction of diazene to ammonia. Importantly, N_2 as a significant source for this ammonia production is ruled out because N_2 was quantified in the assay vials and the concentration was far too low to account for any substantial ammonia production. Likewise, it was possible to rule out the possibility that ammonia was produced by nitrogenase reduction of hydrazine as a diazene breakdown product. Again, hydrazine concentrations were determined in the diazene assay and were found to be too low to account for the ammonia production by nitrogenase. Further, hydrazine reduction is not inhibited by H_2, whereas the ammonia production in the diazene assay was inhibited by H_2. These results provide strong evidence that diazene itself is a substrate for nitrogenase.

Mechanistic Implications of Diazene as a Substrate. The simplest way to explain the behavior of diazene as a nitrogenase substrate is that diazene enters the normal N_2 reduction reaction pathway at a step associated with a semireduced diazene-species bound to FeMo-cofactor (eq 2). Several observations presented here support this model. First is the observation that nitrogenase reduces diazene to ammonia at rates that are comparable to the rate of N_2 reduction itself. The estimated specific activity found here for diazene reduction by nitrogenase of 400 nmol of NH_3/min/mg of MoFe protein is comparable to the specific activity of 600 nmol of NH_3/min/mg of MoFe protein observed for N_2 reduction (*35*). Importantly, this activity for diazene reduction represents a lower limit, as the actual concentration of diazene in solution is lower than the azodiformate concentration because of loss through decomposition. Thus, the true specific activity for diazene reduction will be higher than 400 nmol of NH_3/min/mg of MoFe protein. The observed specific activity for diazene reduction is further minimized by the competition for binding and electrons coming from the diazene breakdown products hydrazine and N_2. Likewise, the value, $K_m \sim 4.5$ mM, estimated for diazene clearly is an upper limit, with the true value being lower for the same reasons put forward above.

A second important observation that implies that diazene enters the normal N_2 reduction pathway at an early step is the inhibition of diazene reduction by H_2. Proton reduction yielding H_2 (called H_2 evolution) is an essential reaction in the nitrogenase mechanism (*43*). H_2 is a competitive inhibitor of N_2 reduction by nitrogenase, but does not inhibit the reduction of any other substrate (except N_2O) (*55*). This inhibition of N_2 reduction by H_2 indicates a unique relationship between H_2 and N_2. The special role of H_2 in the nitrogenase mechanism is further reflected by the fact that, in the absence of another substrate, nitrogenase directs all electron flux to the reduction of protons, yielding H_2. The addition of N_2 to the reaction competes for electron flux

going to proton reduction, thus dramatically lowering H_2 evolution rates. However, H_2 evolution by nitrogenase cannot be eliminated by increasing amounts of N_2, with a minimum stoichiometry of 1 H_2 evolved to 1 N_2 reduced (eq 1), even at high N_2 concentrations (*56*). This has been interpreted to indicate that, when N_2 binds to FeMo-cofactor, it must displace a bound H_2, thus accounting for the fixed stoichiometry (*43*). Further connection between the interactions of N_2 and H_2 with nitrogenase comes from the so-called "HD exchange reaction". Nitrogenase will catalyze the formation of HD when presented with D_2, but only if N_2 is also present (*57*).

Different models haven been put forward (*1*) to explain these intricate interactions between N_2 and H_2, and they share the common feature that H_2 and N_2 interact with FeMo-cofactor at early steps along the N_2 reaction pathway (eq 2). The fact that H_2 does not inhibit the reduction of hydrazine by nitrogenase is consistent with such models if hydrazine is presumed to enter the nitrogenase N_2-reduction reaction pathway at a late stage (eq 2). An alternative explanation would be that diazene and N_2 are reduced at the same specific site on FeMo-cofactor, whereas the reduction of other substrates (e.g., hydrazine and acetylene) might occur at a different specific site (e.g., a different metal) on FeMo-cofactor (*19*, *58*). However, taken together, the present findings that diazene is reduced to ammonia by nitrogenase *and* that both diazene and N_2 reduction are inhibited by H_2 indicate that diazene and N_2 are reduced at the same location and that diazene enters the normal nitrogenase reaction pathway at an early step (eq 2).

Trapping a Diazene-Derived State. To gain insights into the nature of diazene reduction by nitrogenase, we sought to capture and characterize a state with a diazene-derived species bound to FeMo-cofactor. Our earlier work localized a single Fe−S face in the middle of FeMo-cofactor (Fe atoms 2, 3, 6, and 7) as a site for interaction with both alkyne and nitrogenous substrates (Figure 1) (*10*, *36*, *44*, *59*). Two observations from those studies are important to the present effort. First, the size of substrates gaining access to FeMo-cofactor can be controlled by the size of the side chain of the MoFe protein α-70 amino acid residue (*54*). That the wild-type Val at this position significantly limits larger substrates' access to the active site is shown by the result that substitution of α-70^{Val} by the smaller side chain amino acid, Ala, allows substantially larger molecules to act as substrates for nitrogenase. Thus, propyne and hydrazine become much better substrates in the α-70^{Ala} MoFe protein when compared to the wild-type (α-70^{Val}) MoFe protein (*35*, *54*). A second important observation relevant to trapping a diazene-derived species on FeMo-cofactor is the critical role of α-195^{His} (located near the same FeS face, Figure 1) in delivery of protons during the reduction of nitrogenous substrates. This is indicated by the observation that substitution of this residue by glutamine significantly lowers N_2- (*52*) and hydrazine- (*36*) reduction rates, while essentially leaving proton and acetylene reduction rates unchanged. Further, it was also shown that hydrazine and methyldiazene reduction is interrupted in the α-195^{Gln} MoFe protein, allowing an intermediate state to be trapped by rapidly freezing this MoFe protein variant during turnover with these substrates (*27*, *49*).

When the α-195^{Gln} MoFe protein is rapidly frozen during turnover using diazene as substrate, a partial conversion of the resting state FeMo-cofactor $S = {}^3/_2$ EPR signal to a new $S = {}^1/_2$ spin state signal is observed. Prompted by the earlier findings with the α-70^{Ala} MoFe protein, we then used the doubly substituted MoFe protein (α-70^{Ala}/α-195^{Gln}), and found that it was possible to freeze-trap a state that contains a diazene-derived species bound to FeMo-cofactor at relatively high concentration.

The EPR spectrum of this intermediate shares many similarities with EPR spectra observed for the hydrazine-trapped state: similar *g*-values, and dependences of EPR signal intensity on microwave power and temperature (*36*). Overlaying the X- and Q-band EPR spectra for the hydrazine- and diazene-dependent intermediates suggests that they represent the same intermediate, with slightly different populations of two conformational substates. More definitively, ^{15}N- and ^{1}H-ENDOR spectra of the diazene- and hydrazine-dependent states show that they contain substrate-derived [$-NH_x$] species bound to FeMo-cofactor whose characteristics are identical. Each shows a ^{15}N-ENDOR signal from a single (type of) ^{15}N, and the spectra match precisely (Figure 9A). Likewise the ^{1}H-ENDOR spectra match precisely (Figure 9B), with each showing a resolved nonexchangeable signal with $A \sim 4$ MHz, and an exchangeable signal with $A \sim 8-9$ MHz.

The equivalence of the EPR and ^{15}N,^{1}H-ENDOR spectra for the diazene- and hydrazine-dependent states can be explained in three different ways: (i) Diazene could first decompose to hydrazine, and then the resulting hydrazine could react with the MoFe protein, being trapped in the same state as accumulates when hydrazine is used as a substrate; (ii) diazene could be reduced by nitrogenase to the same intermediate state that is trapped when hydrazine is presented as the substrate; and (iii) the diazene- and hydrazine-dependent states could represent different species bound to FeMo-cofactor, but with such similar properties for the bound [$-NH_x$] fragment that these differences are not reflected in the EPR or ^{15}N-ENDOR spectra.

Possibility (i) is ruled out because the majority of the EPR signal observed for nitrogenase trapped during turnover with diazene can be assigned to diazene rather than to a diazene breakdown product (Figure 7). If alternative (ii) applies, it would mean that the diazene-dependent intermediate is generated by enzymatic reduction of diazene, not, for example, merely by binding of diazene in a possibly nonproductive fashion. In other words, the enzyme has reduced the diazene substrate enough that it has "caught up" to the hydrazine-derived species trapped during turnover with hydrazine. As hydrazine, and now diazene, are bona fide substrates that are reduced to NH_3, this would then mean that both of these substrates in fact access the same, productive, mechanistic pathway to NH_3 that is used by N_2, thereby validating the hypothesis embodied in (eq 2), which implies that nitrogenase functions through an alternating mechanism, rather than a distal mechanism (*27*).

We consider (iii) to be possible only if the bound [$-NH_x$] has the same value of *x* for both intermediates. If *x* were different for the two intermediates, then the bound N would be hybridized differently: for example, sp^2 if diazene itself were bound in the diazene-dependent intermediate; sp^3 if hydrazine were bound in the hydrazine intermediate. This would mean that the nitrogen orbitals involved in binding

to M have different orbital compositions in the two states ($^1/_3$ 2s for sp^2, $^1/_4$ 2s for sp^3). However, this would be expected to lead to different hyperfine couplings, contrary to the results presented here. While further experiments are required to definitively distinguish between alternatives (ii) and (iii), possibility (ii) seems the most likely explanation.

In summary, through *in situ* generation of diazene we have demonstrated that wild-type nitrogenase reduces diazene to ammonia. The reductions of both N_2 and diazene are inhibited by H_2, indicating that N_2 and diazene are reduced at the same specific site on FeMo-cofactor and that diazene enters at an early step in the same reaction pathway. An EPR-active state has been trapped during turnover of an α-70^{Ala}/α-195^{Gln} MoFe protein variant with diazene, and ^{15}N,^1H-ENDOR has established that this state incorporates an [$-NH_x$] moiety bound to FeMo-cofactor that is indistinguishable from the [$-NH_x$] moiety bound to FeMo-cofactor in the hydrazine state trapped during turnover with hydrazine. An important consequence of the studies presented here is that diazene is highly likely to join the normal N_2-reduction pathway, and thus the diazene- and hydrazine-trapped states are likely to represent intermediates in the normal reduction of N_2, as postulated by alternating mechanisms for reduction of N_2 by nitrogenase. Further characterization of these two trapped states is expected to provide insights into their nature and thus to shed further light on the nitrogenase N_2-reduction mechanism.

ACKNOWLEDGMENT

The authors thank Dr. Graham Palmer for guidance in the *in situ* synthesis of diazene.

SUPPORTING INFORMATION AVAILABLE

Additional figures illustrating the microwave power dependence of the X- and Q-band EPR spectra and the pH dependence of the EPR spectra. This material is available free of charge via the Internet at http://pubs.acs.org.

REFERENCES

1. Burgess, B. K., and Lowe, D. J. (1996) The mechanism of molybdenum nitrogenase, *Chem. Rev. 96*, 2983−3011.
2. Howard, J. B., and Rees, D. C. (1996) Structural basis of biological nitrogen fixation, *Chem. Rev. 96*, 2965−2982.
3. Smil, V. (2001) *Enriching the Earth: Fritz Haber, Carl Bosch, and the Transformation of World Food Production*, MIT Press, Cambridge, MA.
4. Georgiadis, M. M., Komiya, H., Chakrabarti, P., Woo, D., Kornuc, J. J., and Rees, D. C. (1992) Crystallographic structure of the nitrogenase iron protein from *Azotobacter vinelandii*, *Science 257*, 1653−1659.
5. Seefeldt, L. C., and Dean, D. R. (1997) Role of nucleotides in nitrogenase catalysis, *Acc. Chem. Res. 30*, 260−266.
6. Howard, J. B., and Rees, D. C. (1994) Nitrogenase: A nucleotide-dependent molecular switch, *Annu. Rev. Biochem. 63*, 235−264.
7. Hageman, R. V., and Burris, R. H. (1978) Nitrogenase and nitrogenase reductase associate and dissociate with each catalytic cycle, *Proc. Natl. Acad. Sci. U.S.A. 75*, 2699−2702.
8. Orme-Johnson, W. H., and Münck, E. (1980) On the prosthetic groups of nitrogenase, in *Molybdenum and molybdenum containing enzymes* (Coughlan, M. P., Ed.) pp 427−438, Pergamon Press, Oxford.
9. Seefeldt, L. C., Dance, I., and Dean, D. R. (2004) Substrate interactions with nitrogenase: Fe versus Mo, *Biochemistry 43*, 1401−1409.
10. Dos, Santos, P. C., Igarashi, R. Y., Lee, H. I., Hoffman, B. M., Seefeldt, L. C., and Dean, D. R. (2005) Substrate Interactions with the nitrogenase active site, *Acc. Chem. Res. 38*, 208−214.
11. Thorneley, R. N. F., Eady, R. R., and Lowe, D. J. (1978) Biological nitrogen fixation by way of an enzyme-bound dinitrogen-hydride intermediate, *Nature 272*, 557−558.
12. Dance, I. (1996) Theoretical investigations of the mechanism of biological nitrogen fixation at the FeMo cluster site, *J. Biol. Inorg. Chem. 1*, 581−586.
13. Hinnemann, B., and Nørskov, J. K. (2004) Chemical activity of the nitrogenase FeMo cofactor with a central nitrogen ligand: Density functional study, *J. Am. Chem. Soc. 126*, 3920−3927.
14. Rod, T. H., Hammer, B., and Nørskov, J. K. (1999) Nitrogen adsorption and hydrogenation on a $MoFe_6S_9$ complex, *Phys. Rev. Lett. 82*, 4054−4057.
15. Stavrev, K. K., and Zerner, M. C. (1998) Studies on the hydrogenation steps of the nitrogen molecule at the *Azotobacter vinelandii* nitrogenase site, *Int. J. Quant. Chem. 70*, 1159−1168.
16. Deng, H., and Hoffmann, R. (1993) How N_2 might be activated by the FeMo-cofactor in nitrogenase, *Angew. Chem., Int. Ed. Engl. 32*, 1062−1065.
17. Kastner, J., Hemmen, S., and Blochl, P. E. (2005) Activation and protonation of dinitrogen at the FeMo cofactor of nitrogenase, *J. Chem. Phys. 123*, 074306.
18. Durrant, M. C. (2002) An atomic-level mechanism for molybdenum nitrogenase. Part 1. Reduction of dinitrogen, *Biochemistry 41*, 13934−13945.
19. Huniar, U., Ahlrichs, R., and Coucouvanis, D. (2004) Density functional theory calculations and exploration of a possible mechanism of N_2 reduction by nitrogenase, *J. Am. Chem. Soc. 126*, 2588−2601.
20. Fryzuk, M. D., and MacKay, B. A. (2004) Dinitrogen coordination chemistry: On the biomimetic borderlands, *Chem. Rev. 104*, 385−401.
21. Chatt, J., Dilworth, J. R., Richards, R. L., and Sanders, J. R. (1969) Chemical evidence concerning the function of molybdenum in nitrogenase, *Nature 224*, 1201−1202.
22. Chatt, J., Dilworth, J. R., and Richards, R. L. (1978) Recent advances in the chemistry of nitrogen fixation, *Chem. Rev. 78*, 589−625.
23. Pickett, C. J. (1996) The Chatt cycle and the mechanism of enzymic reduction of molecular nitrogen, *J. Biol. Inorg. Chem. 1*, 601−606.
24. Yandulov, D. V., and Schrock, R. R. (2003) Catalytic reduction of dinitrogen to ammonia at a single molybdenum center, *Science 301*, 76−78.
25. Schrock, R. R. (2003) Catalytic reduction of dinitrogen under mild conditions, *Chem. Commun.* 2389−2391.
26. Schrock, R. R. (2005) Catalytic reduction of dinitrogen to ammonia at well defined single metal sites, *Phil. Trans. R. Soc. A 363*, 959−969.
27. Barney, B. M., Lukoyanov, D., Yang, T. C., Dean, D. R., Hoffman, B. M., and Seefeldt, L. C. (2006) A methyldiazene ($HN{=}N\text{-}CH_3$) derived species bound to the nitrogenase active site FeMo-cofactor: implications for mechanism, *Proc. Natl. Acad. Sci. U.S.A. 103*, 17113−17118.
28. Davis, L. C. (1980) Hydrazine as a substrate and inhibitor of *Azotobacter vinelandii* nitrogenase, *Arch. Biochem. Biophys. 204*, 270−276.
29. Malinak, S. M., Simeonov, A. M., Mosier, P. E., McKenna, C. E., and Coucouvanis, D. (1997) Catalytic reduction of cis-dimethyldiazene by the $[MoFe_3S_4]^{(3+)}$ clusters. The four-electron reduction of a N═N bond by a nitrogenase-relevant cluster and implications for the function of nitrogenase, *J. Am. Chem. Soc. 119*, 1662−1667.
30. McKenna, C. E., Simeonov, A. M., Eran, H., and Bravo-Leerahhandh, M. (1996) Reduction of cyclic and acyclic diazene derivatives by *Azotobacter vinelandii* nitrogenase: diazirine and trans-dimethyldiazene, *Biochemistry 35*, 4502−4514.
31. Christiansen, J., Goodwin, P. J., Lanzilotta, W. N., Seefeldt, L. C., and Dean, D. R. (1998) Catalytic and biophysical properties of a nitrogenase apo-MoFe protein produced by a *nifB*-deletion mutant of *Azotobacter vinelandii*, *Biochemistry 37*, 12611−12623.
32. Liao, G. L., and Palmer, G. (1998) Diazene—a not so innocent ligand for the binuclear center in cytochrome c oxidase, *Biochemistry 37*, 15583−15592.
33. Audrieth, D. C., and Mohr, E. B. (1953) Biurea, *Inorg. Syntheses 4*, 26−28.
34. Hristova-Kazmierski, M. K., and Kepler, J. A. (1999) Synthesis of [14C]azodicarbonamide, *J. Labelled Compd. Radiopharm. 42*, 203−206.

35. Barney, B. M., Igarashi, R. Y., Dos, Santos, P. C., Dean, D. R., and Seefeldt, L. C. (2004) Substrate interaction at an iron-sulfur face of the FeMo-cofactor during nitrogenase catalysis, *J. Biol. Chem. 279*, 53621−53624.
36. Barney, B. M., Laryukhin, M., Igarashi, R. Y., Lee, H. I., Dos Santos, P. C., Yang, T. C., Hoffman, B. M., Dean, D. R., and Seefeldt, L. C. (2005) Trapping a hydrazine reduction intermediate on the nitrogenase active site, *Biochemistry 44*, 8030−8037.
37. Davoust, C. E., Doan, P. E., and Hoffman, B. M. (1996) Q-band pulsed electron spin-echo spectrometer and its application to ENDOR and ESEEM, *J. Magn. Reson. 119*, 38−44.
38. Mims, W. B. (1965) Pulsed ENDOR experiments, *Proc. R. Soc. London 238*, 452−457.
39. Hoffman, B. M., DeRose, V. J., Doan, P. E., Gurbiel, R. J., Houseman, A. L. P., and Telser, J. (1993) Metalloenzyme active-site structure and function through multifrequency CW and pulsed ENDOR, in *Biol. Magn. Reson.* (Berliner, L. J., and Reuben, J., Eds.) pp 151−218, Plenum Press, New York.
40. Doan, P. E., and Hoffman, B. M. (1997) Making hyperfine selection in Mims ENDOR independent of deadtime, *Chem. Phys. Lett. 269*, 208−214.
41. Stanbury, D. M. (1991) Kinetic behavior of diazene in aqueous solutions, *Inorg. Chem. 30*, 1293−1296.
42. Guth, J. H., and Burris, R. H. (1983) Inhibition of nitrogenase catalyzed NH_3 formation by H_2, *Biochemistry 22*, 5111−5122.
43. Thorneley, R. N. F., and Lowe, D. J. (1985) Kinetics and mechanisms of the nitrogenase enzyme system, in *Molybdenum Enzymes* (Spiro, T. G., Ed.) pp 221−284, Wiley, New York.
44. Benton, P. M. C., Laryukhin, M., Mayer, S. M., Hoffman, B. M., Dean, D. R., and Seefeldt, L. C. (2003) Localization of a substrate binding site on FeMo-cofactor in nitrogenase: trapping propargyl alcohol with an α-70-substituted MoFe protein, *Biochemistry 42*, 9102−9109.
45. Davis, L. C., Henzl, M. T., Burris, R. H., and Orme-Johnson, W. H. (1979) Iron-sulfur clusters in the molybdenum-iron protein component of nitrogenase. Electron paramagnetic resonance of the carbon monoxide inhibited state, *Biochemistry 18*, 4860−4869.
46. Pollock, C. R., Lee, H.-I., Cameron, L. M., DeRose, V. J., Hales, B. J., Orme-Johnson, W. H., and Hoffman, B. M. (1995) Investigation of CO bound to inhibited forms of nitrogenase MoFe protein by ^{13}C ENDOR, *J. Am. Chem. Soc. 117*, 8686−8687.
47. Sørlie, M., Christiansen, J., Dean, D. R., and Hales, B. J. (1999) Detection of a new radical and FeMo-cofactor EPR signal during acetylene reduction by the α-H195Q mutant of nitrogenase, *J. Am. Chem. Soc. 121*, 9457−9458.
48. Lee, H. I., Sørlie, M., Christiansen, J., Song, R., Dean, D. R., Hales, B. J., and Hoffman, B. M. (2000) Characterization of an intermediate in the reduction of acetylene by nitrogenase α-Gln195 MoFe protein by Q-band EPR and ^{13}C, ^{1}H ENDOR, *J. Am. Chem. Soc. 122*, 5582−5587.
49. Barney, B. M., Yang, T. C., Igarashi, R. Y., Dos, Santos, P. C., Laryukhin, M., Lee, H. I., Hoffman, B. M., Dean, D. R., and Seefeldt, L. C. (2005) Intermediates trapped during nitrogenase reduction of N_2, CH_3-N=NH, and H_2N-NH_2, *J. Am. Chem. Soc. 127*, 14960−14961.
50. Smith, B. E., Lowe, D. J., and Bray, R. C. (1972) Nitrogenase of *Klebsiella pneumoniae*: Electron-paramagnetic-resonance studies on the catalytic mechanism, *Biochem. J. 130*, 641−643.
51. Smith, B. E., Lowe, D. J., and Bray, R. C. (1973) Studies by electron paramagnetic resonance on the catalytic mechanism of nitrogenase of *Klebsiella pneumoniae*, *Biochem. J. 135*, 331−341.
52. Kim, C. H., Newton, W. E., and Dean, D. R. (1995) Role of the MoFe protein alpha-subunit histidine-195 residue in FeMo-cofactor binding and nitrogenase catalysis, *Biochemistry 34*, 2798−2808.
53. Fisher, K., Dilworth, M. J., and Newton, W. E. (2000) Differential effects on N_2 binding and reduction, HD formation, and azide reduction with alpha-195His- and alpha-191Gln-substituted MoFe proteins of *Azotobacter vinelandii* nitrogenase, *Biochemistry 39*, 15570−15577.
54. Mayer, S. M., Niehaus, W. G., and Dean, D. R. (2002) Reduction of short chain alkynes by a nitrogenase alpha-70Ala-substituted MoFe protein, *J. Chem. Soc., Dalton Trans. 5*, 802−807.
55. Jensen, B. B., and Burris, R. H. (1986) N_2O as a substrate and as a competitive inhibitor of nitrogenase, *Biochemistry 25*, 1083−1088.
56. Simpson, F. B., and Burris, R. H. (1984) A nitrogen pressure of 50 atmoshperes does not prevent evolution of hydrogen by nitrogenase, *Science 224*, 1095−1097.
57. Li, J., and Burris, R. H. (1983) Influence of pN_2 and pD_2 on HD formation by various nitrogenases, *Biochemistry 22*, 4472−4480.
58. Dance, I. (2004) The mechanism of nitrogenase. Computed details of the site and geometry of binding of alkyne and alkene substrates and intermediates, *J. Am. Chem. Soc. 126*, 11852−11863.
59. Igarashi, R. Y., Dos, Santos, P. C., Niehaus, W. G., Dance, I. G., Dean, D. R., and Seefeldt, L. C. (2004) Localization of a catalytic intermediate bound to the FeMo-cofactor of nitrogenase, *J. Biol. Chem. 279*, 34770−34775.

BI062294S